Serine 182 on RORγt regulates T helper 17 and regulatory T cell functions to resolve inflammation

Shengyun Ma[1], Shefali Patel[2], Nicholas Chen[1], Parth R. Patel[1], Benjamin S. Cho[1], John T. Chang[2], Wendy Jia Men Huang[1,*]

[1] Department of Cellular and Molecular Medicine,

University of California San Diego, La Jolla, CA 92093, U.S.A

[2] Department of Medicine,

University of California San Diego, La Jolla, CA 92093, U.S.A

* Corresponding author

ABSTRACT

Unresolved inflammation causes tissue damage and contributes to autoimmune conditions. However, the molecules and mechanisms controlling T cell-mediated inflammation remain to be fully elucidated. Here, we report an unexpected role of the RAR-Related Orphan Receptor-gamma protein (RORγt) in resolving tissue inflammation. Single-cell RNA-seq (scRNA-seq) revealed that an evolutionarily conserved serine 182 residue on RORγt (RORγt^{S182}) is critical for restricting IL-1β-mediated Th17 activities and promoting anti-inflammatory cytokine IL-10 production in RORγt^{+} Treg cells in inflamed tissues. Phospho-null RORγt^{S182A} knock-in mice experienced delayed recovery and succumbed to exacerbate diseases after dextran sulfate sodium (DSS) induced colitis and experimental autoimmune encephalomyelitis (EAE) challenge. Together, these results highlight the essential role of RORγt^{S182} in resolving T cell-mediated tissue inflammation, providing a potential therapeutic target to combat autoimmune diseases.

INTRODUCTION

RAR-Related Orphan Receptor-gamma (RORγ) is an evolutionarily conserved member of the nuclear receptor transcription factor family. The long isoform (RORγ) is broadly expressed in liver, kidney, and muscles, and the shorter isoform (RORγt) is uniquely found in cells of the immune system (Jetten and Joo, 2006). Both isoforms are encoded by the *RORC* locus. Humans with mutations of *RORC* have impaired anti-bacterial and anti-fungal immunity (Okada et al., 2015). Previous genetic studies in mouse models identified critical roles of RORγt in preventing apoptosis of $CD4^+CD8^+$ double positive T cells during positive selection in the thymus (Guo et al., 2016; Sun et al., 2000), facilitating secondary lymphoid tissue organogenesis (Cherrier et al., 2012), as well as driving the differentiation of effector T lymphocyte and innate lymphoid cells (ILCs) involved in mucosal protection (Ciofani et al., 2012; Ivanov et al., 2006; Scoville et al., 2016). More importantly, RORγt also regulates the effector T cell gene programs implicated in the pathogenesis of autoimmune diseases, including the production of interleukin 17 (IL-17) cytokines in pathogenic T helper 17 (Th17) cells and IL-10 in regulatory T cells (Tregs); both have been shown to be dysregulated in patients with inflammatory bowel diseases (IBD) (Fujino et al., 2003; Ivanov et al., 2006; Jiang et al., 2014; Neumann et al., 2014; Sun et al., 2019). However, the mechanisms by which RORγt control cell-type-specific transcription programs are not well understood, thus, limiting our ability to target this pathway to ameliorate autoimmune problems without adversely affecting other homeostatic processes that are also highly dependent on RORγt.

RORγt and its transcriptional functions are regulated by post-transcriptional modifications (PTMs), including acetylation, ubiquitination, and phosphorylation (Rutz et al., 2016). While acetylation of RORγt by p300 impairs RORγt binding to chromatin DNA and its target gene expression, deacetylation of RORγt mediated by SIRT1, restores the ability of RORγt to drive *Il17a* expression *(Lim et al., 2015)*. Ubiquitination at Lys69 on RORγt is selectively required for Th17 differentiation and dispensable for T cell development (He et al., 2017a). RORγt poly-ubiquitination and deubiquitination by E3 ubiquitin ligases (UBR5 and ITCH) and deubiquitinating enzyme A (DUBA), respectively, define the rate of RORγt proteasomal degradation (Kathania et al., 2016; Rutz et al., 2015). Phosphorylation of RORγt at S376 and S484 are found to stimulate and inhibit RORγt functions in cultured Th17 cells, respectively (He et al., 2017b). In addition, phosphorylation of RORγt at S489 promotes RORγt interaction with AhR and subsequently enhanced IL-17A production during autoimmune responses (Chuang et al., 2018). However, little is known about the function of those different PTMs contribute to the diverse RORγt function *in vivo*, especially phosphorylation.

Here, we report that RORγt is phosphorylated at S182. Single-cell RNA-seq (scRNA-seq) revealed that RORγt^{S182} not only restricts IL-1β-mediated Th17 cell effector functions, but also promotes anti-inflammatory cytokine IL-10 production in lymphoid tissue (LT)-like RORγt^{+} Treg cells in inflamed tissues. Phosphor-null RORγt^{S182A} knock-in mice experienced delayed recovery and succumbed to more severe disease after DSS induced colitis and EAE challenges.

RESULTS

Serine 182 of RORγt is dispensable for T cell development in the thymus

To characterize post-translational modifications (PTMs) of RORγt, a 2xFlag-tagged murine RORγt expression construct was transfected into HEK293ft cells. Whole-cell lysates after transfection 48hrs were used for anti-Flag immunoprecipitation and tandem mass-spectrometry (MS/MS) analysis. Peptide mapping to RORγt harbored phosphorylation at S182, T197, S489, methylation at R185, and ubiquitination at K495 (Figure 1A). In particular, the serine residue in position 182 of RORγt or 203 of RORγ, was conserved between mouse and human (Figure S1A). Phosphorylation at this site was the most abundant among all the RORγt PTMs identified (Figure 1B), consistent with previous reports (He et al., 2017b; Huttlin et al., 2010). To assess the *in vivo* function of this serine residue, we generated phospho-null knock-in mice (RORγt^{S182A}) by replacing the serine codon on *Rorc* with that of alanine using CRISPR-Cas9 technology (Figure 1C). Heterozygous crosses yielded wildtype (WT) and homozygous RORγt^{S182A} littermates born in Mendelian ratio with similar growth rates (Figure S1B).

In the thymus, CD4$^+$CD8$^+$ thymocytes express RORγt to maintain high levels of the anti-apoptotic factor, B-cell lymphoma-extra large (Bcl-xL). RORγt total knockout thymocytes undergo apoptosis, resulting in the impaired generation of mature T cells (Sun et al., 2000). In RORγt^{S182A} CD4$^+$CD8$^+$ thymocytes, RORγt and Bcl-xL protein abundance were similar to those observed in WT cells (Figure S1C-D). RORγt^{S182A} CD4$^+$CD8$^+$ double-positive thymocytes matured normally into single positive CD4$^+$ T helper and CD8$^+$ cytotoxic T cells (Figure S1E). In the spleen, mature CD4$^+$ T helper and CD8$^+$ cytotoxic

cell populations also appeared normal in the RORγt^{S182A} mice (Figure S1F). Together, these results suggest that S182 of RORγt and/or its phosphorylation is dispensable for T cell development.

scRNA-seq revealed RORγt^{S182} dependent Th17 and Treg populations in steady state colon

In the intestinal lamina propria, RORγt acts as a master transcription factor regulating differentiation and effector cytokine production in several immune cell populations, including RORγt^{+}Foxp3^{-} (Th17), RORγt^{+}Foxp3^{+} T cells (RORγt^{+} Treg), and type 3 innate lymphoid cells (ILC3) (Cai et al., 2011; Ivanov et al., 2006; Song et al., 2015). Similar proportion of RORγt-expressing CD4^{+} T cells and ILC3 (CD3^{-}) cells were present in both the small intestine and colon of WT and RORγt^{S182A} mice (Figure S1G-H). Since IBDs primarily affect the colon, we characterized the contribution of RORγt^{S182} to the colonic CD4^{+} T cell transcriptome using scRNA-seq (10x Genomics). Colonic lamina propria CD4^{+} T cells from two pairs of WT and RORγt^{S182A} mice were captured using anti-CD4 magnetic beads (Figure 1D). From each sample, 10-13,000 cells were sequenced. A total of 11,725 cells with *Cd4*>0.4 and ~1100 genes/cell were analyzed using Seraut (Stuart et al., 2019).

UMAP (uniform manifold approximation and projection) projection revealed 12 cell clusters with distinct gene expression patterns in our dataset. Our subsequent analysis focused on 8175 cells (69.7% total) in clusters 0-3 and 5-6; consisting of cells with high expression of CD4 and Cd3e (Figure 1E-F). Cells in clusters 0 and 3 had marked expression of *Il17a* and *Ifng*, representing two distinct subsets of the Th17 lineage. Cells

in cluster 2 with the high level of *Foxp3* and *Il10* were regulatory T cells. Memory cells (cluster 1, *Cd44*^{hi}) and naive cells (cluster 5, *Cd44*^{low}) had abundant expressions of *Klf2*, *Tcf7*, and *Ccr7*. Proliferating CD4^{+} T cells (cluster 6) had high levels of *Stmn1* and *Ki67* (Figure 1G). At the population level, there was a significant reduction of Treg cells (cluster 2) and an increase in one of the Th17 subsets (cluster 3) in the RORγt^{S182A} colon (Figure 1H). Results from the scRNA-seq analyses reveal an unexpected dependency of Th17 and Treg populations on RORγt^{S182} in the steady state of colon.

RORγt^{S182A} augmented IL-17A production in response to IL-1β

Differential gene expression analysis revealed Th17 cells in cluster 0 and cluster 3 shared a common gene program but also harbored unique surface receptor and effector cytokine expression patterns (Figure 2A-B). Th17 cells in cluster 0 expressed greater *Il18r1*, *Il1rn*, *Ccl2, Ccl5, Ccl7, Ccl8*, *Cxcl1, and Cxcl13.* In contrast, Th17 cells in cluster 3 had higher levels of *Il23r*, *Ccr6*, *Il22*, *Ccl20,* and *Cxcl3*. Intriguingly, Th17 cells in cluster 3 from the RORγt^{S182A} colon had higher expression of *Il1r1* (Figure 2C). The *Il1r1* gene encodes the IL-1β receptor involves in promoting inflammatory cytokine production in Th17 cells and contributes to pathologies in Th17-mediated autoimmunity (Coccia et al., 2012; Sutton et al., 2006). We therefore speculated that Th17 cells in cluster 3 from the RORγt^{S182A} colon with higher *Il1r1* expression would have enhanced Th17 cytokine production potential. Indeed, Th17 cells in cluster 3 from the RORγt^{S182A} colon had higher expression of *Il17a* (Figure 2C).

Next, we wanted to determine whether S182 on RORγt contributes to IL-17A production in Th17 cells downstream of IL-1β receptor signaling in a T cell-intrinsic

manner. Naive T cells from WT and RORγt^{S182A} mice were purified and polarized toward the Th17 lineage *in vitro* as described (Ciofani et al., 2012) (diagramed in Figure 3A). In the presence of IL-1β, RORγt^{S182A} Th17 cells had significantly greater IL-17A production potential (Figure 3B and S2A). Similar RORγt protein abundance was found in WT and RORγt^{S182A} Th17 cells (Figure 3C). Western analysis confirmed that RORγt proteins were phosphorylated at S182 in cultured Th17 WT cells (Figure 3D). RT-qPCR confirmed that an increase of *Il17a* at the RNA level was observed in RORγt^{S182A} Th17 cells cultured in the presence of IL-6, IL-23, and IL-1β (Figure 3E); this culture combination is the classic pathogenic Th17 culture condition (Ghoreschi et al., 2010). Chromatin immunoprecipitation (ChIP-seq) experiments indicated that RORγt binding on the *Il17a-Il17f* locus in WT and RORγt^{S182A} Th17 cells were comparable (Figure 3F). However, higher H3K27 acetylation (H3K27ac) was detected at the CNS4 regulatory region in RORγt^{S182A} Th17 cells (Figure 3F). Together, these results reveal the unexpected role of RORγt^{S182} in negatively regulating Th17 effector cytokine production in the presence of IL-1β (modeled in Figure 3G).

RORγt^{S182A} T cells drive exacerbated diseases in two models of colitis

Previous reports suggest that Th17 cells generated in the presence of IL-6, IL-23, and IL-1β contribute to autoimmune pathologies in the intestine (El-Behi et al., 2011; Ghoreschi et al., 2010). Therefore, we hypothesized that RORγt^{S182A} Th17 cells with hyperresponsiveness to IL-1β receptor signaling will drive tissue inflammation. In a model of T cell transfer colitis, Rag1$^{-/-}$ recipients, lacking endogenous T cells, received WT or RORγt^{S182A} donor CD4^{+} naive T cells, experienced similar weight loss between day 2-16.

However, the weights of recipients of WT cells stabilized on day 19-31, but those with RORγt^{S182A} cells experienced further weight reduction (Figure 4A). RT-qPCR confirmed the increases of *Il17a and Il1r1* at the RNA level (Figure 4B). These results indicate that the contribution of S182 on RORγt and/or its phosphorylation to colonic inflammation is CD4$^+$ T cell-intrinsic.

We also challenged the WT and RORγt^{S182A} cohoused littermates with 2% DSS in the drinking water to induce acute intestinal epithelial injury, a model with disease pathologies similar to those observed in human ulcerative colitis patients (Chassaing et al., 2014). In this model, scRNA-seq experiment of colonic lamina propria cells from WT mice harvested on day 10 post DSS challenge in a workflow similar to the steady state experiment described earlier in Figure 1D revealed that *Il1b* was upregulated in CD4$^+$ T cell-associated macrophages (cluster 4) and neutrophils (cluster 10) (Figure S4A-B). In the T cell compartment, DSS challenged colon harbored an increase of memory (cluster 1) and Treg (cluster 2) cells, and a reduction of Th17 (cluster 3) (Figure S4C-D). The DSS-responsive genes in Th17 cells (cluster 0 and 3 depicted in Figure S4C) were enriched with tumor necrosis factor-alpha (TNF) and oxidative phosphorylation signatures (Figure S4E), which are pivotal pathways previously implicated in colitis (Koelink et al., 2020; Liu et al., 2017). Consistent with our findings in the T cell transfer colitis model, DSS challenged RORγt^{S182A} mice had a significant delay in weight recovery on day 8-10 as compared to their WT littermates (Figure 4C). Colons harvested from DSS-challenged RORγt^{S182A} mice were much shorter than those from DSS-challenged WT mice (Figure 4D). Colonic CD4$^+$ T cells from the DSS-challenged RORγt^{S182A} mice also harbored elevated surface expression of IL-1β receptors (Figure S3A), implicated in pathogenic

Th17 driven autoimmunity (Cua et al., 2003; Ronchi et al., 2016). Histological analysis revealed significantly more infiltrating immune cells present in the colons from RORγt^{S182A} mice on day 10 (Figure 4E). Together, these *in vivo* results suggest that S182 on RORγt and/or its phosphorylation in CD4$^+$ T cells contribute to inflammation resolution in colitis settings.

scRNA-seq revealed RORγt^{S182}-dependent colonic Th17 and Treg programs during DSS challenge

To characterize the contribution of RORγt^{S182A} to T cell programs during the resolution phase of colonic inflammation, we harvested colonic lamina propria cells from two pairs of WT and RORγt^{S182A} mice on day 10 post DSS challenge for scRNA-seq. At the population level, fewer memory T cells (cluster 1) were found in the DSS-challenged RORγt^{S182A} colons as compared to WT (Figure S5A). Differential gene expression analysis revealed greater number of genes in clusters 0-3 that were upregulated in the DSS-challenge RORγt^{S182A} colon (Figure S5B), suggesting a global repressive role of RORγt^{S182} in colonic T cells in inflamed settings. Notably, RORγt^{S182A} Th17 cells in cluster 0 had higher *Il17a* expression, and cells in cluster 3 had higher pro-inflammatory cytokine *Ccl5* expression (Figure 5A-B). Flow cytometry analysis revealed that the RORγt$^+$Foxp3$^-$ Th17 subset had more IL-17A producers in the DSS-challenged RORγt^{S182A} colon (Figure 5C).

In addition to the notable expansion of IL-17A producing Th17 cells, DSS-challenged RORγt^{S182A} mice also had significantly fewer IL-10 producers among the RORγt$^+$Foxp3$^+$ (RORγt$^+$ Treg) cells (Figure 5C). Recent studies suggested that IL-10

secreted by these cells helps to limit colonic inflammation (Ohnmacht et al., 2015; Sefik et al., 2015; Xu et al., 2018; Yang et al., 2016). To identify the Treg population with RORγt^{S182}-dependent IL-10 production, we further divided the Tregs, in cluster 2, into 5 subsets (Figure 5D). Subsets 0 and 4 express genes characteristics of suppressive Treg cells, including *Gzmb* and *Ccr1* (Figure 5E), as described in previous reports (Miragaia et al., 2019). Subsets 2 and 3 express genes characteristics of lymphoid tissue (LT)-like Treg, including *S1pr1*. Subsets 1 express genes characteristics of non-lymphoid tissues (NLT) Treg, including *Gata3* and *Pdcd1*. The reduction of cluster 2 cell number in the steady state RORγt^{S182A} colon observed in Figure 1H can be traced to the loss of LT-like (subset 3) Tregs (Figure S6A). Upon DSS challenge, IL-10 expression in LT-like (subset 3) Tregs was significantly reduced in the RORγt^{S182A} colon (Figure 5F-G), consistent with our observation in Figure 5C. Altogether, these data indicate that RORγt^{S182} negatively regulates effector cytokine production in Th17 cells, promotes expression of anti-inflammation cytokine, IL-10, as well as epithelial repair factors in RORγt^{+} Treg cells to facilitate inflammation resolution during colitis.

RORγt^{S182A} mice experienced the more severe disease in EAE

Finally, we assessed whether S182 of RORγt is involved in the negative regulation of inflammation beyond intestinal mucosal injury. Previous reports suggest that pathogenic Th17 cells drive disease in the EAE mouse model (Thakker et al., 2007) by secreting IL-17A to recruit CD11c^{+} dendritic cells (DC) and further promoting IL-17A production from bystander TCRγδ^{+} type 17 (Tγδ17) cells to fuel local inflammation (Cua et al., 2003; Ivanov et al., 2006; Solt et al., 2011; Xiao et al., 2014); modeled in Figure 6A. When challenged

in our model, RORγt^{S182A} mice had higher disease scores and experienced greater weight loss (Figure 6B-C). Total spinal cord immune infiltrates in RORγt^{S182A} mice had higher levels of *Cd4*, *Cd11c*, and *Il17a* mRNAs (Figure 6D-E). Flow cytometry results further confirmed a significant increase in the number of IL-17A producing Th17 (CD4$^+$TCRγδ$^-$) and Tγδ17 (CD4$^-$TCRγδ$^+$) cells (Figure 6F), as well as DC (CD11c$^+$) cells, but no change in macrophages (CD11b$^+$F4/80$^+$), in the spinal cord of the RORγt^{S182A} mice (Figure 6G). Overall, these results demonstrate the critical role of S182 on RORγt in modulating RORγt$^+$ T cell functions to protect against colonic mucosal inflammation and central nervous system autoimmune pathologies.

DISCUSSION

Our study revealed the transcriptional landscapes of colonic lamina propria CD4$^+$ T cells in homeostasis and during colitis at the single-cell level. In addition to the naive and memory populations, we identified two novel subsets of Th17 and five subsets of Treg cells with distinct cell surface receptors and effector molecule expressions. Colonic Th17 cells in cluster 3 express higher levels of inflammation-related signature genes, including *Il23r*. Under steady state, mutation of S182 on RORγt resulted in an expansion of this Th17 subset in the colon. During the inflammation resolution phase, post DSS challenge, cells in this cluster were significantly reduced. In contrast, colonic Th17 cells in cluster 0 enriched with *Il18r1*, *Il1rn*, *Ccl2, Ccl5, Ccl7, Ccl8*, *Cxcl1, and Cxcl13* may help to establish chemotactic gradients to regulate trafficking of local immune cells. Interestingly, DSS-regulated genes of Th17 cells in cluster 0 were highly enriched in TNF and NFκB signaling pathways. TNF antagonists have been the mainstay in the treatment of inflammatory

bowel diseases (IBD) for over 20 years (Vulliemoz et al., 2020), and the NFκB pathway is known to be activated in inflamed colonic tissue from IBD patients (Atreya et al., 2008; Liu et al., 2017). It would be interesting for future studies to explore whether Th17 cells subset in cluster 0 is targeted by anti-TNF therapies in human IBD.

In the RORγt^{S182A} colon, both Th17 subsets had elevated expression of *Il1r1*, resulting in augmented IL-17A production in response to IL-1β signaling. In a positive feedforward loop, IL-17A stimulates the production of IL-1β by neutrophils and monocytes (McGinley et al., 2020), which in turn signals on T cells to potentiate intestinal inflammatory response and encephalomyelitis in the central nervous system (Coccia et al., 2012; Sutton et al., 2006). As a result, RORγt^{S182A} mice with Th17 that are hyperresponsive to IL-1β signaling had delayed recovery when challenged with DSS-induced gut injury and succumbed to more severe pathology during EAE. These results highlight the novel repressive function of S182 on RORγt in dampening IL-17A production in response to IL-1β signaling in Th17 cells.

During the inflammation resolution phase post-DSS challenge, we also observed an increase of colonic Treg (cluster 2) cells. S182 on RORγt is required for maintaining LT-like (Cluster 2 subset 3) Treg population in steady state colon and their IL-10 production potential during DSS-induced colitis. RORγt^{+} Tregs are abundantly found in the intestinal mucosa and peripheral lymphoid organs (Ohnmacht et al., 2015; Sefik et al., 2015). Secretion of IL-10 by these cells helps to protect against autoimmune diseases (Coquet et al., 2013; Ohnmacht et al., 2015; Rutz et al., 2015; Sefik et al., 2015; Xu et al., 2018) by dampening uncontrolled production of inflammatory cytokines, including IL-17A, and excessive intestinal inflammation in mouse models (Guo, 2016). Impaired IL-10

production has been associated with severe cases of inflammatory bowel diseases patients (Ishizuka et al., 2001; Saxena et al., 2015), and several studies suggest that administration of IL-10 in these patients as a potential therapy (Ishizuka et al., 2001; Saxena et al., 2015). In DSS-treated RORγt^{S182A} mice, IL-10 producing LT-like Tregs had increased expression of *S1pr4*, which is involved in cell migration *(Olesch et al., 2017),* as well as decreased levels of *Cd44* and *Id2*, encoding molecules implicated in Treg activation and IL-10 production (Bollyky et al., 2009; Hwang et al., 2018). Future studies will be needed to investigate whether RORγt^{S182}-dependent IL-10 expressions in LT-like Tregs exert paracrine effects on local Th17 effector programs and contribute to the delayed DSS and EAE disease recovery observed in RORγt^{S182A} mice. Furthermore, it remained to be explored whether the same or distinct kinase(s) and/or pathways are involved in phosphorylating S182 on RORγt in these different T cell subsets.

Given the essential role of RORγt in the differentiation and function of Th17 cells implicated in autoimmunity, many RORγt inhibitors have been developed for therapeutic purposes. Most current inhibitors are designed to disrupt RORγt-dependent transcription by preventing its interaction with steroid receptor coactivators. Unfortunately, as this is a common mechanism RORγt employs across the different cell and tissue types, this approach will likely exert undesired side-effects on thymic development and other innate immune cells expressing RORγt. Our discovery of the unique involvement of S182 on RORγt in regulating colonic mucosal Th17 and Treg populations and functions, but dispensable for thymocyte development, provide a new cell-type-specific venue for designing better therapies to combat T cell-mediated inflammatory diseases.

FIGURE LEGEND

Figure 1. **scRNA-seq revealed RORγt^{S182}-dependent Th17 and Treg populations in steady state colon**.

A. Proportion of modified and unmodified peptides identified by Tandem MS/MS mapping to murine RORγt from whole cell lysates of 293ft cells transfected with Flag2x-mRORγt expression construct for 48hrs.

B. Top: Major phosphorylation sites in relation to the activation function (AF-1), DNA-binding domain (DBD), and ligand-binding domain (LBD) of RORγt. Bottom: representative mass spectral map of one murine RORγt peptide carrying a phosphorylated S182 residue.

C. CRISPR-Cas mediated genomic mutations to generate the RORγt^{S182A} knock-in mice.

D. scRNA-seq experiment workflow: CD4^{+} and their associated colonic lamina propria cells were enriched with anti-CD4 microbeads. 10X Genomics droplet-based 3′ scRNA-seq was employed to reveal captured cell transcript profiles.

E. UMAP plot of twelve immune cell clusters obtained from D (left) and the average expression of *Cd3e* in each cell (right).

F. Heatmap of average expression of genes with cluster-specific expression patterns from E.

G. Violin plots of selected genes from each cluster, with gene expression scaled on the y-axis.

H. Proportions of colonic CD4^{+} T cells in each cluster from two pairs of WT and RORγt^{S182A} littermates.

Figure 2. **scRNA-seq identified two subsets of Th17 cells in steady state colon.**

A. Left: zoom in view of the UMAP plot showing two neighboring populations of colonic Th17 cells in red (cluster 0) and green (cluster 3). Right: select cell surface receptors and effector molecules enriched in the two Th17 subsets from WT mice.
B. Heatmap of mean scaled average expression of cluster-specific genes in steady colonic Th17 (cluster 0 and 3) and Treg (cluster 2) cells of WT and RORγt^{S182A}.
C. Expression of *Il17a* and *Il1r1* in colonic Th17 cell subsets (cluster 0 and 3) in the steady state WT and RORγt^{S182A} mice. UMAP expression plots (left) and violin plots (right).

Figure 3. **IL-1β signaling promoted dysregulated effector cytokine production in RORγt^{S182A} Th17 cells.**

A. Th17 culture workflow *in vitro*.
B. Proportion of IL-17A^{+}IL-17F^{+} producers among Th17 cells cultured for 3 days under conditions as indicated. Each dot represents result from one mouse. * p-value<0.05, ** p-value<0.01 (paired t-test).
C. Geometric mean fluorescence (gMFI) of RORγt in WT and RORγt^{S182A} Th17 cells cultured under different conditions. Each dot represents result from one mouse.
D. Western blot analysis of total RORγt and S182-phosphorylated RORγt in cultured Th17 cells from two pairs of WT and RORγt^{S182A} littermates.
E. Normalized *Il17a* mRNA expression in WT and RORγt^{S182A} Th17 cells cultured in IL-6, IL-1β and IL-23 for 3 days, detected by qRT-PCR. Each dot represents result from one mouse. * p-value<0.05 (paired t-test).

F. Top: IGV browser showing RORγt and p300 occupancy at *Il17a-Il17f* locus as reported previously (Ciofani et al., 2012) along with the location of ChIP-qPCR primers designed to capture each of the conserved non-coding regulatory elements (CNS). Bottom: Enrichment of RORγt and H3K27ac at the *Il17a-Il17f* locus in WT and RORγt^{S182A} Th17 cells as determined by ChIP-qPCR. n=4, ** p<0.01 (t-test).

G. Working model: IL-1β signaling promotes dysregulated effector cytokines production in RORγt^{S182A} Th17 cells.

Figure 4. **RORγt^{S182A} T cells drived exacerbated diseases in two models of colitis.**

A. Weight changes of Rag1$^{-/-}$ mice receiving WT or RORγt^{S182A} naive CD4^{+} T cells. Each dot represents result from one mouse. ** p-value<0.01 and *** p-value<0.001 (multiple t-test).

B. Expression level of *Il1r1*, *Il23r* and *Il17a* in colonic lamina propria of Rag1$^{-/-}$ mice receiving WT or RORγt^{S182A} naive CD4^{+} T cells. Each dot represents result from one mouse. * p-value<0.05 (t-test).

C. Weight changes of WT and RORγt^{S182A} mice challenged with 2% DSS in drinking water for 7 days and monitored for another 3 days. Each dot represents result from one mouse. * p-value<0.05 (multiple t-test).

D. Top: representative bright field images of colons from C. Bottom: summarized colonic lengths of DSS treated WT and RORγt^{S182A} mice from C harvested on day 10. Each dot represents result from one mouse. ** p-value<0.01 (t-test).

E. Top: representative colonic sections from D. Bottom: summarized score of colonic inflammatory infiltrates (bottom) in DSS treated WT and RORγt^{S182A} mice. Each dot represents result from one mouse. * p-value<0.05 (t-test).

Figure 5. **scRNA-seq revealed RORγt^{S182}-dependent colonic Th17 and Treg programs during DSS challenge.**

A. Heatmap of Log_2 fold change of select RORγt^{S182}-dependent genes expression in Th17 (cluster 0 and 3) and Treg (cluster 2) from steady state and DSS challenged colons.
B. Violin plots of the selected gene expressions in Th17 (cluster 0 and 3) and Treg (cluster 2) cells.
C. Top: representative flow cytometry analysis. Bottom: proportion of IL-10 and IL-17A production potential in colonic RORγt^{+}Foxp3^{-} (Th17), RORγt^{+}Foxp3^{+} (RORγt^{+} Treg), RORγt^{-}Foxp3^{+} (Treg), and RORγt^{-}Foxp3^{-} cells from DSS treated WT and RORγt^{S182A} mice and harvested on day 10. Each dot represents result from one mouse. * p-value<0.05, *** p-value<0.001 (t-test).
D. Closed up UMAP of the five Treg subsets within Cluster 2.
E. Heatmap of mean scaled average expression of select Treg subsets enriched genes from D.
F. Percentage of cells expressing RORγt^{S182}-dependent genes (grey, p-Value<0.05) in colonic Treg subsets 0 and 3 from DSS challenged WT and RORγt^{S182A} mice. Select genes were labeled and highlighted in blue.

G. Left: UMAP displaying *Il10* expression in scRNA-seq dataset. Right: violin plots of the *Il10* expression in LT-like Treg (subset 3) cells from control or DSS challenged WT and RORγt^{S182A} mice.

Figure 6. **RORγt^{S182A} mice experienced more severe disease in EAE model.**

A. Working hypothesis: RORγt^{S182} acts as the upstream negative regulator of pathogenic Th17 cell activities in EAE.
B. Disease score of MOG-immunized WT (n=7) and RORγt^{S182A} (n=14) mice. Results were combined of three independent experiments. ** p-value<0.01, *** p-value<0.001 (multiple t-test).
C. Weight change of MOG-immunized WT and RORγt^{S182A} mice. Results were combined of three independent experiments. * p-value<0.05, *** p-value<0.001 (multiple t-test).
D. Normalized mRNA expression of *Cd4*, *Cd11c*, *Cd19* and *Cd11b* in spinal cords infiltrated at the peak of EAE disease (day 16-19) from MOG-immunized WT and RORγt^{S182A} mice as detected by qRT-PCR. Each dot represents result from one mouse. * p-value<0.05 (paired t-test).
E. Normalized mRNA expression of the indicated cytokine genes in spinal cords infiltrated at the peak of EAE disease (day16-19) from MOG-immunized WT and RORγt^{S182A} EAE mice as detected by qRT-PCR. Each dot represents result from one mouse. * p-value<0.05 (paired t-test).

F. Number of total T helper ($CD4^+$) and $TCR\gamma\delta^+$ (left) and $IL\text{-}17A^+$ expressing Th17 and $T\gamma\delta17$ cells (right) in EAE mice harvested at the peak of disease (day16-19). Each dot represents result from one mouse. * p-value<0.05 (t-test).

G. $CD11b^+F4/80^+$ (macrophage, left) and $CD3e^-CD11c^+$ (DC, right) cells numbers in the spinal cords of EAE mice harvested at the peak of disease (day16-19). Each dot represents result from one mouse. * p-value<0.05 (t-test).

Supplementary Figure S1. **Normal thymic T cell development and intestine homeostasis in RORγt^{S182A} mice**.

A. S182 (black line) localizing to the hinge region of RORγt is conserved between mouse and human.

B. Weight of WT (n=49) and RORγt^{S182A} (n=57) mice assessed at the indicated ages. Each dot represents result from one mouse.

C. Geometric mean fluorescent intensity (GMFI) of RORγt in thymic $CD4^+CD8\alpha^+$ double positive (DP) cells from WT and RORγt^{S182A} cohoused littermates. Each dot represents result from one mouse.

D. Representative histogram of Bcl-xL expression in thymic DP cells from WT and RORγt^{S182A} mice. This experiment was repeated three times on independent biological samples with similar results.

E. Representative flow cytometry analysis of CD4 and CD8a expression in thymic cells from WT and RORγt^{S182A} mice. This experiment was repeated three times on independent biological samples with similar results.

F. Representative flow cytometry analysis of CD4 and CD8α expression in splenocytes from WT and RORγt^{S182A} mice. This experiment was repeated three times on independent biological samples with similar results.

G. Proportion of RORγt^{+}Foxp3^{-}, RORγt^{+}Foxp3^{+}, and RORγt^{-}Foxp3^{+} T cell subsets and CD3e^{-}RORγt^{+}Foxp3^{-} (ILC3) cells in the steady state small intestinal lamina propria of WT (n=6) and RORγt^{S182A} mice (n=6).

H. Proportion of RORγt^{+}Foxp3^{-}, RORγt^{+}Foxp3^{+}, and RORγt^{-}Foxp3^{+} T cell subsets and CD3e^{-}RORγt^{+}Foxp3^{-} ILC3 cells in the steady state colonic lamina propria of WT (n=6) and RORγt^{S182A} mice (n=6).

Supplementary Figure S2. **Representative cytokine production potential in Th17 cells cultured from WT and RORγt^{S182A} mice.**

A. Representative flow cytometry analysis of IL-17A and IL-17F expression in cultured Th17 cells from WT and RORγt^{S182A} mice as described in Figure 3B.

Supplementary Figure S3**. Cell surface IL-1R expression on colonic Th17 cells in steady state and DSS-challenged WT and RORγt^{S182A} mice.**

A. Summary of proportions of IL-1R^{+} Th17 cells in colonic lamina propria of WT and RORγt^{S182A} mice treated with or without DSS (left) and representative flow plots (right). Each dot represents result from one mouse. * p-value<0.05 (paired t-test).

Supplementary Figure S4. **DSS-induced epithelial injury altered colonic immune cell populations and their transcription programs in WT mice.**

A. UMAP plot of colonic lamina propria cells obtained from steady state (blue) and day 10 post DSS challenged (red) WT mice.
B. Left: violin plot of select genes enriched in $CD4^+$ T cells associated macrophages (cluster 4) and neutrophils (cluster 10). Right: average expression of *Il1b* in macrophages and neutrophiles from control and DSS challenged WT mice.
C. Altered proportions of each $CD4^+$ T cell cluster in colonic lamina propria cells from steady state (n=2) and day 10 post DSS treated WT mice (n=2).
D. DSS-dependent genes (p-value<0.05) identified in each cell cluster.
E. Heatmap of $-Log_{10}$ *p*-Value of the top seven KEGG pathways from DSS-dependent genes in clusters 0,1, 2, 3, and 5.

Supplementary Figure S5**. RORγt^{S182}-dependent cell populations and target genes in colon under steady state and during DSS challenge.**

A. Proportions of individual scRNA-seq clusters among colonic lamina propria $CD4^+$ T cells from DSS-challenged WT and RORγt^{S182A} mice. * p-value<0.05, n=2.
B. Number of RORγt^{S182}-dependent genes in individual scRNA-seq clusters from steady state (control) (left) and DSS-challenged (right) WT and RORγt^{S182A} mice (n=2). # of DE genes means number of differentially expressed genes.

Supplementary Figure S6**. Cluster 2 Treg subsets in control and DSS challenged WT and RORγt^{S182A} mice**

A. Proportions of Treg subclusters from steady state (top) and DSS-treated (bottom) colons of WT (n=2) and RORγt^{S182A} mice (n=2). * p-value<0.05 (multiple t-test).

METHODS

Mice

RORγt^{S182A} were generated by CRISPR-Cas9 technology in the C57BL/6 (Jackson Laboratories) background mice and confirmed by sanger sequencing of the *Rorc* locus. Heterozygous mice were bred to yield 8-12 WT and homogenous knock-in (RORγt^{S182A}) cohoused littermates for paired experiments. Rag1$^{-/-}$ (Jackson Laboratory stock No: 002216) were obtained from Dr. John Chang's Laboratory. Adult mice at least eight weeks old were used. All animal studies were approved and followed the Institutional Animal Care and Use Guidelines of the University of California San Diego.

Th17 cell culture

Mouse naive T cells were purified from spleens and lymph nodes of 8-12 weeks old mice using the Naive CD4+ T Cell Isolation Kit according to the manufacturer's instructions (Miltenyi Biotec). Cells were cultured in Iscove's Modified Dulbecco's Medium (IMDM, Sigma Aldrich) supplemented with 10% heat-inactivated FBS (Peak Serum), 50U/50 ug penicillin-streptomycin (Life Technologies), 2 mM glutamine (Life Technologies), and 50 μM β-mercaptoethanol (Sigma Aldrich). For polarized Th17 cell polarization, naive cells were seeded in 24-well or 96-well plates, pre-coated with rabbit anti-hamster IgG, and cultured in the presence of 0.25 μg/mL anti-CD3ε (eBioscience), 1 μg/mL anti-CD28 (eBioscience), 20 ng/mL IL-6 (R&D Systems), and/or 0.1 ng/mL TGF-β (R&D Systems), 20 ng/mL IL-1β (R&D Systems), 25 ng/mL IL-23 (R&D Systems) for 72 hours.

DSS induced and T cell transfer colitis

Dextran Sulfate Sodium Salt (DSS) Colitis Grade 36,000-59,000MW (MP Biomedicals) was added to the drinking water at a final concentration of 2% (wt/vol) and administered for 7 days. Mice were weighed every other day. On day 10, colons were collected for H&E staining and lamina propria cells were isolation as described (Lefrancois and Lycke, 2001). Cells were kept for RNA isolation or flow cytometry. The H&E slides from each sample were scored in a double-blind fashion as described previously (Abbasi et al., 2020). For T cell transfer model of colitis, 0.5 million naive $CD4^+$ T cells isolated from mouse splenocytes using the Naive $CD4^+$ T Cell Isolation Kit (Miltenyi), as described above, were injected intraperitoneally into $Rag1^{-/-}$ recipients. Mice weights were measured twice a week. Pathology scoring of distal colons from DSS-challenged mice were performed blind following previously published guidelines (Koelink et al., 2018).

scRNA-seq and analysis

Colonic lamina propria cells from DSS or non-DSS treated mice were collected and enriched for $CD4^+$ T cells using the mouse $CD4^+$ T cell Isolation Kit (Miltenyi). Enriched $CD4^+$ cells (~10,000 per mouse) were prepared for single cell libraries using the Chromium Single Cell 3' Reagent Kit (10xGenomics). The pooled libraries of each sample (20,000 reads/cell) were sequenced on one lane of NovaSeq S4 following manufacturer's recommendations.

Cellranger v3.1.0 was used to filter, align, and count reads mapped to the mouse reference genome (mm10-3.0.0). The Unique Molecular Identifiers (UMI) count matrix obtained was used for downstream analysis using Seurat (v4.0.1). The cells with

mitochondrial counts >5%, as well as outlier cells in the top and bottom 0.2% of the total gene number detected index were excluded. After filtering, randomly selected 10,000 cells per sample were chosen for downstream analysis. Cells with *Cd4* expression lower than 0.4 were removed, resulting in 27,420 total cells from eight samples. These cells were scaled and normalized using log-transformation, and the top 3,000 genes were selected for principal component analysis. The dimensions determined from PCA were used for clustering and non-linear dimensional reduction visualizations (UMAP). Differentially expressed genes identified by FindMarkers were used to characterize each cell cluster. Other visualization methods from Seurat such as VlnPlot, FeaturePlot, and DimPlot were also used.

EAE model

EAE was induced in 8-week-old mice by subcutaneous immunization with 100 µg myelin oligodendrocyte glycoprotein (MOG35–55) peptide (GenScript Biotech) emulsified in complete Freund's adjuvant (CFA, Sigma-Aldrich), followed by administration of 400 ng pertussis toxin (PTX, Sigma-Aldrich) on days 0 and 2 as described in (Bittner et al., 2014). Clinical signs of EAE were assessed as follows: 0, no clinical signs; 1, partially limp tail; 2, paralyzed tail; 3, hind limb paresis; 4, one hind limb paralyzed; 5, both hind limbs paralyzed; 6, hind limbs paralyzed, weakness in forelimbs; 7, hind limbs paralyzed, one forelimb paralyzed; 8, hind limb paralyzed, both forelimbs paralyzed; 9, moribund; 10, death.

Flow cytometry

Cells were stimulated with 5 ng/mL Phorbol 12-myristate 13-acetate (PMA, Millipore Sigma) and 500ng/mL ionomycin (Millipore Sigma) in the presence of GoligiStop (BD Bioscience) for 5 hours at 37˚C, followed by cell surface marker staining. Fixation/Permeabilization buffers (eBioscience) were used per manufacturer instructions to assess intracellular transcription factor and cytokine expression. Antibodies are listed in Table S1.

cDNA synthesis, qRT-PCR, and RT-PCR

Total RNA was extracted with the RNeasy kit (QIAGEN) and reverse transcribed using iScript™ Select cDNA Synthesis Kit (Bio-Rad Laboratories). Real time RT-PCR was performed using iTaq™ Universal SYBR® Green Supermix (Bio-Rad Laboratories). Expression data was normalized to *Gapdh* mRNA levels. Primer sequences are listed in Table S2.

Chromatin immunoprecipitation

ChIP was performed on 5-10 million Th17 cells crosslinked with 1% formaldehyde. Chromatin was sonicated and immunoprecipitated using antibodies listed in Table S1 and captured on Dynabeads (ThermoFisher Scientific). Immunoprecipitated protein-DNA complexes were reverse cross-linked and chromatin DNA purified as described in (Kaikkonen et al., 2013). ChIP primer sequences are listed in Table S2.

Statistical analysis

All values are presented as means ± SD. Significant differences were evaluated using GraphPad Prism 8 software. The Student's t-test or paired t-test were used to determine significant differences between two groups. A two-tailed p-value of <0.05 was considered statistically significant in all experiments.

AUTHOR CONTRIBUTIONS

S.M. designed and performed *in vivo*, *in vitro* and scRNA-seq studies with the help of N.C. scRNA-seq study was analyzed by S.P. with input from J.T.C and W.J.M.H. S.M. and B.S.C. completed the DSS colitis studies. P.R.P. completed the double-blinded histology scoring of the colonic sections from DSS challenged mice. J.T.C. supervised the scRNA-seq analysis by S.P., contributed resources, and edited the manuscript. W.J.M.H. wrote the manuscript together with S.M.

ACKNOWLEDGEMENTS

S.M., N.C., B.S.C., P.R.P, and W.J.M.H. were partially funded by the Edward Mallinckrodt, Jr. Foundation and the National Institutes of Health (NIH) (R01 GM124494 to WJM Huang). Illumina sequencing was conducted at the IGM Genomics Center, University of California San Diego, with support from NIH (S10 OD026929). The Moores Cancer Center Histology Core conducted colonic tissue sectioning and staining with support from NIH (P30 CA23100). We thank Karen Sykes for suggestions to the manuscript.

CONFLICT OF INTEREST

All authors declare no competing financial interests.

REFERENCE

Abbasi, N., Long, T., Li, Y., Yee, B.A., Cho, B.S., Hernandez, J.E., Ma, E., Patel, P.R., Sahoo, D., Sayed, I.M., *et al.* (2020). DDX5 promotes oncogene C3 and FABP1 expressions and drives intestinal inflammation and tumorigenesis. Life Sci Alliance *3*.

Atreya, I., Atreya, R., and Neurath, M.F. (2008). NF-kappaB in inflammatory bowel disease. J Intern Med *263*, 591-596.

Bittner, S., Afzali, A.M., Wiendl, H., and Meuth, S.G. (2014). Myelin oligodendrocyte glycoprotein (MOG35-55) induced experimental autoimmune encephalomyelitis (EAE) in C57BL/6 mice. J Vis Exp.

Bollyky, P.L., Falk, B.A., Long, S.A., Preisinger, A., Braun, K.R., Wu, R.P., Evanko, S.P., Buckner, J.H., Wight, T.N., and Nepom, G.T. (2009). CD44 costimulation promotes FoxP3+ regulatory T cell persistence and function via production of IL-2, IL-10, and TGF-beta. J Immunol *183*, 2232-2241.

Cai, Y., Shen, X., Ding, C., Qi, C., Li, K., Li, X., Jala, V.R., Zhang, H.G., Wang, T., Zheng, J., *et al.* (2011). Pivotal role of dermal IL-17-producing gammadelta T cells in skin inflammation. Immunity *35*, 596-610.

Chassaing, B., Aitken, J.D., Malleshappa, M., and Vijay-Kumar, M. (2014). Dextran sulfate sodium (DSS)-induced colitis in mice. Curr Protoc Immunol *104*, Unit 15 25.

Cherrier, M., Sawa, S., and Eberl, G. (2012). Notch, Id2, and RORgammat sequentially orchestrate the fetal development of lymphoid tissue inducer cells. J Exp Med *209*, 729-740.

Chuang, H.C., Tsai, C.Y., Hsueh, C.H., and Tan, T.H. (2018). GLK-IKKbeta signaling induces dimerization and translocation of the AhR-RORgammat complex in IL-17A induction and autoimmune disease. Sci Adv *4*, eaat5401.

Ciofani, M., Madar, A., Galan, C., Sellars, M., Mace, K., Pauli, F., Agarwal, A., Huang, W., Parkhurst, C.N., Muratet, M., *et al.* (2012). A validated regulatory network for Th17 cell specification. Cell *151*, 289-303.

Coccia, M., Harrison, O.J., Schiering, C., Asquith, M.J., Becher, B., Powrie, F., and Maloy, K.J. (2012). IL-1beta mediates chronic intestinal inflammation by promoting the accumulation of IL-17A secreting innate lymphoid cells and CD4(+) Th17 cells. J Exp Med *209*, 1595-1609.

Coquet, J.M., Middendorp, S., van der Horst, G., Kind, J., Veraar, E.A., Xiao, Y., Jacobs, H., and Borst, J. (2013). The CD27 and CD70 costimulatory pathway inhibits effector function of T helper 17 cells and attenuates associated autoimmunity. Immunity *38*, 53-65.

Cua, D.J., Sherlock, J., Chen, Y., Murphy, C.A., Joyce, B., Seymour, B., Lucian, L., To, W., Kwan, S., Churakova, T., *et al.* (2003). Interleukin-23 rather than interleukin-12 is the critical cytokine for autoimmune inflammation of the brain. Nature *421*, 744-748.

El-Behi, M., Ciric, B., Dai, H., Yan, Y., Cullimore, M., Safavi, F., Zhang, G.X., Dittel, B.N., and Rostami, A. (2011). The encephalitogenicity of T(H)17 cells is dependent on IL-1- and IL-23-induced production of the cytokine GM-CSF. Nat Immunol *12*, 568-575.

Fujino, S., Andoh, A., Bamba, S., Ogawa, A., Hata, K., Araki, Y., Bamba, T., and Fujiyama, Y. (2003). Increased expression of interleukin 17 in inflammatory bowel disease. Gut *52*, 65-70.

Ghoreschi, K., Laurence, A., Yang, X.P., Tato, C.M., McGeachy, M.J., Konkel, J.E., Ramos, H.L., Wei, L., Davidson, T.S., Bouladoux, N., *et al.* (2010). Generation of pathogenic T(H)17 cells in the absence of TGF-beta signalling. Nature *467*, 967-971.

Guo, B. (2016). IL-10 Modulates Th17 Pathogenicity during Autoimmune Diseases. J Clin Cell Immunol *7*.

Guo, Y., MacIsaac, K.D., Chen, Y., Miller, R.J., Jain, R., Joyce-Shaikh, B., Ferguson, H., Wang, I.M., Cristescu, R., Mudgett, J.*, et al.* (2016). Inhibition of RORgammaT Skews TCRalpha Gene Rearrangement and Limits T Cell Repertoire Diversity. Cell Rep *17*, 3206-3218.

He, Z., Ma, J., Wang, R., Zhang, J., Huang, Z., Wang, F., Sen, S., Rothenberg, E.V., and Sun, Z. (2017a). A two-amino-acid substitution in the transcription factor RORgammat disrupts its function in TH17 differentiation but not in thymocyte development. Nat Immunol *18*, 1128-1138.

He, Z., Wang, F., Zhang, J., Sen, S., Pang, Q., Luo, S., Gwack, Y., and Sun, Z. (2017b). Regulation of Th17 Differentiation by IKKalpha-Dependent and -Independent Phosphorylation of RORgammat. J Immunol *199*, 955-964.

Huttlin, E.L., Jedrychowski, M.P., Elias, J.E., Goswami, T., Rad, R., Beausoleil, S.A., Villen, J., Haas, W., Sowa, M.E., and Gygi, S.P. (2010). A tissue-specific atlas of mouse protein phosphorylation and expression. Cell *143*, 1174-1189.

Hwang, S.M., Sharma, G., Verma, R., Byun, S., Rudra, D., and Im, S.H. (2018). Inflammation-induced Id2 promotes plasticity in regulatory T cells. Nat Commun *9*, 4736.

Ishizuka, K., Sugimura, K., Homma, T., Matsuzawa, J., Mochizuki, T., Kobayashi, M., Suzuki, K., Otsuka, K., Tashiro, K., Yamaguchi, O.*, et al.* (2001). Influence of interleukin-10 on the interleukin-1 receptor antagonist/interleukin-1 beta ratio in the colonic mucosa of ulcerative colitis. Digestion *63 Suppl 1*, 22-27.

Ivanov, II, McKenzie, B.S., Zhou, L., Tadokoro, C.E., Lepelley, A., Lafaille, J.J., Cua, D.J., and Littman, D.R. (2006). The orphan nuclear receptor RORgammat directs the differentiation program of proinflammatory IL-17+ T helper cells. Cell *126*, 1121-1133.

Jetten, A.M., and Joo, J.H. (2006). Retinoid-related Orphan Receptors (RORs): Roles in Cellular Differentiation and Development. Adv Dev Biol *16*, 313-355.

Jiang, W., Su, J., Zhang, X., Cheng, X., Zhou, J., Shi, R., and Zhang, H. (2014). Elevated levels of Th17 cells and Th17-related cytokines are associated with disease activity in patients with inflammatory bowel disease. Inflamm Res *63*, 943-950.

Kaikkonen, M.U., Spann, N.J., Heinz, S., Romanoski, C.E., Allison, K.A., Stender, J.D., Chun, H.B., Tough, D.F., Prinjha, R.K., Benner, C.*, et al.* (2013). Remodeling of the enhancer landscape during macrophage activation is coupled to enhancer transcription. Mol Cell *51*, 310-325.

Kathania, M., Khare, P., Zeng, M., Cantarel, B., Zhang, H., Ueno, H., and Venuprasad, K. (2016). Itch inhibits IL-17-mediated colon inflammation and tumorigenesis by ROR-gammat ubiquitination. Nat Immunol *17*, 997-1004.

Koelink, P.J., Bloemendaal, F.M., Li, B., Westera, L., Vogels, E.W.M., van Roest, M., Gloudemans, A.K., van 't Wout, A.B., Korf, H., Vermeire, S.*, et al.* (2020). Anti-TNF therapy in IBD exerts its therapeutic effect through macrophage IL-10 signalling. Gut *69*, 1053-1063.

Koelink, P.J., Wildenberg, M.E., Stitt, L.W., Feagan, B.G., Koldijk, M., van 't Wout, A.B., Atreya, R., Vieth, M., Brandse, J.F., Duijst, S.*, et al.* (2018). Development of Reliable, Valid and Responsive Scoring Systems for Endoscopy and Histology in Animal Models for Inflammatory Bowel Disease. J Crohns Colitis *12*, 794-803.

Lefrancois, L., and Lycke, N. (2001). Isolation of mouse small intestinal intraepithelial lymphocytes, Peyer's patch, and lamina propria cells. Curr Protoc Immunol *Chapter 3*, Unit 3 19.

Lim, H.W., Kang, S.G., Ryu, J.K., Schilling, B., Fei, M., Lee, I.S., Kehasse, A., Shirakawa, K., Yokoyama, M., Schnolzer, M.*, et al.* (2015). SIRT1 deacetylates RORgammat and enhances Th17 cell generation. J Exp Med *212*, 973.

Liu, T., Zhang, L., Joo, D., and Sun, S.C. (2017). NF-kappaB signaling in inflammation. Signal Transduct Target Ther *2*.

McGinley, A.M., Sutton, C.E., Edwards, S.C., Leane, C.M., DeCourcey, J., Teijeiro, A., Hamilton, J.A., Boon, L., Djouder, N., and Mills, K.H.G. (2020). Interleukin-17A Serves a Priming Role in Autoimmunity by Recruiting IL-1beta-Producing Myeloid Cells that Promote Pathogenic T Cells. Immunity *52*, 342-356 e346.

Miragaia, R.J., Gomes, T., Chomka, A., Jardine, L., Riedel, A., Hegazy, A.N., Whibley, N., Tucci, A., Chen, X., Lindeman, I.*, et al.* (2019). Single-Cell Transcriptomics of Regulatory T Cells Reveals Trajectories of Tissue Adaptation. Immunity *50*, 493-504 e497.

Neumann, C., Heinrich, F., Neumann, K., Junghans, V., Mashreghi, M.F., Ahlers, J., Janke, M., Rudolph, C., Mockel-Tenbrinck, N., Kuhl, A.A.*, et al.* (2014). Role of Blimp-1 in programing Th effector cells into IL-10 producers. Journal of Experimental Medicine *211*, 1807-1819.

Ohnmacht, C., Park, J.H., Cording, S., Wing, J.B., Atarashi, K., Obata, Y., Gaboriau-Routhiau, V., Marques, R., Dulauroy, S., Fedoseeva, M.*, et al.* (2015). The microbiota regulates type 2 immunity through ROR gamma t(+) T cells. Science *349*, 989-993.

Okada, S., Markle, J.G., Deenick, E.K., Mele, F., Averbuch, D., Lagos, M., Alzahrani, M., Al-Muhsen, S., Halwani, R., Ma, C.S.*, et al.* (2015). IMMUNODEFICIENCIES. Impairment of immunity to Candida and Mycobacterium in humans with bi-allelic RORC mutations. Science *349*, 606-613.

Olesch, C., Ringel, C., Brune, B., and Weigert, A. (2017). Beyond Immune Cell Migration: The Emerging Role of the Sphingosine-1-phosphate Receptor S1PR4 as a Modulator of Innate Immune Cell Activation. Mediators Inflamm *2017*, 6059203.

Ronchi, F., Basso, C., Preite, S., Reboldi, A., Baumjohann, D., Perlini, L., Lanzavecchia, A., and Sallusto, F. (2016). Experimental priming of encephalitogenic Th1/Th17 cells requires pertussis toxin-driven IL-1beta production by myeloid cells. Nat Commun *7*, 11541.

Rutz, S., Eidenschenk, C., Kiefer, J.R., and Ouyang, W. (2016). Post-translational regulation of RORgammat-A therapeutic target for the modulation of interleukin-17-mediated responses in autoimmune diseases. Cytokine Growth Factor Rev *30*, 1-17.

Rutz, S., Kayagaki, N., Phung, Q.T., Eidenschenk, C., Noubade, R., Wang, X., Lesch, J., Lu, R., Newton, K., Huang, O.W.*, et al.* (2015). Deubiquitinase DUBA is a post-translational brake on interleukin-17 production in T cells. Nature *518*, 417-421.

Saxena, A., Khosraviani, S., Noel, S., Mohan, D., Donner, T., and Hamad, A.R. (2015). Interleukin-10 paradox: A potent immunoregulatory cytokine that has been difficult to harness for immunotherapy. Cytokine *74*, 27-34.

Scoville, S.D., Mundy-Bosse, B.L., Zhang, M.H., Chen, L., Zhang, X., Keller, K.A., Hughes, T., Chen, L., Cheng, S., Bergin, S.M.*, et al.* (2016). A Progenitor Cell Expressing Transcription Factor RORgammat Generates All Human Innate Lymphoid Cell Subsets. Immunity *44*, 1140-1150.

Sefik, E., Geva-Zatorsky, N., Oh, S., Konnikova, L., Zemmour, D., McGuire, A.M., Burzyn, D., Ortiz-Lopez, A., Lobera, M., Yang, J.*, et al.* (2015). Individual intestinal symbionts induce a distinct population of ROR gamma(+) regulatory T cells. Science *349*, 993-997.

Solt, L.A., Kumar, N., Nuhant, P., Wang, Y., Lauer, J.L., Liu, J., Istrate, M.A., Kamenecka, T.M., Roush, W.R., Vidovic, D.*, et al.* (2011). Suppression of TH17 differentiation and autoimmunity by a synthetic ROR ligand. Nature *472*, 491-494.

Song, C., Lee, J.S., Gilfillan, S., Robinette, M.L., Newberry, R.D., Stappenbeck, T.S., Mack, M., Cella, M., and Colonna, M. (2015). Unique and redundant functions of NKp46+ ILC3s in models of intestinal inflammation. J Exp Med *212*, 1869-1882.

Stuart, T., Butler, A., Hoffman, P., Hafemeister, C., Papalexi, E., Mauck, W.M., 3rd, Hao, Y., Stoeckius, M., Smibert, P., and Satija, R. (2019). Comprehensive Integration of Single-Cell Data. Cell *177*, 1888-1902 e1821.

Sun, M., He, C., Chen, L., Yang, W., Wu, W., Chen, F., Cao, A.T., Yao, S., Dann, S.M., Dhar, T.G.M.*, et al.* (2019). RORgammat Represses IL-10 Production in Th17 Cells To Maintain Their Pathogenicity in Inducing Intestinal Inflammation. J Immunol *202*, 79-92.

Sun, Z., Unutmaz, D., Zou, Y.R., Sunshine, M.J., Pierani, A., Brenner-Morton, S., Mebius, R.E., and Littman, D.R. (2000). Requirement for RORgamma in thymocyte survival and lymphoid organ development. Science *288*, 2369-2373.

Sutton, C., Brereton, C., Keogh, B., Mills, K.H., and Lavelle, E.C. (2006). A crucial role for interleukin (IL)-1 in the induction of IL-17-producing T cells that mediate autoimmune encephalomyelitis. J Exp Med *203*, 1685-1691.

Thakker, P., Leach, M.W., Kuang, W., Benoit, S.E., Leonard, J.P., and Marusic, S. (2007). IL-23 is critical in the induction but not in the effector phase of experimental autoimmune encephalomyelitis. J Immunol *178*, 2589-2598.

Vulliemoz, M., Brand, S., Juillerat, P., Mottet, C., Ben-Horin, S., Michetti, P., and on behalf of Swiss Ibdnet, a.o.w.g.o.t.S.S.o.G. (2020). TNF-Alpha Blockers in Inflammatory Bowel Diseases: Practical Recommendations and a User's Guide: An Update. Digestion *101 Suppl 1*, 16-26.

Xiao, S., Yosef, N., Yang, J., Wang, Y., Zhou, L., Zhu, C., Wu, C., Baloglu, E., Schmidt, D., Ramesh, R.*, et al.* (2014). Small-molecule RORgammat antagonists inhibit T helper 17 cell transcriptional network by divergent mechanisms. Immunity *40*, 477-489.

Xu, M., Pokrovskii, M., Ding, Y., Yi, R., Au, C., Harrison, O.J., Galan, C., Belkaid, Y., Bonneau, R., and Littman, D.R. (2018). c-MAF-dependent regulatory T cells mediate immunological tolerance to a gut pathobiont. Nature *554*, 373-377.

Yang, B.H., Hagemann, S., Mamareli, P., Lauer, U., Hoffmann, U., Beckstette, M., Fohse, L., Prinz, I., Pezoldt, J., Suerbaum, S.*, et al.* (2016). Foxp3(+) T cells expressing RORgammat represent a stable regulatory T-cell effector lineage with enhanced suppressive capacity during intestinal inflammation. Mucosal Immunol *9*, 444-457.

Serine 182 on RORγt regulates T helper 17 and regulatory T cell functions to resolve inflammation

Graphical Abstract

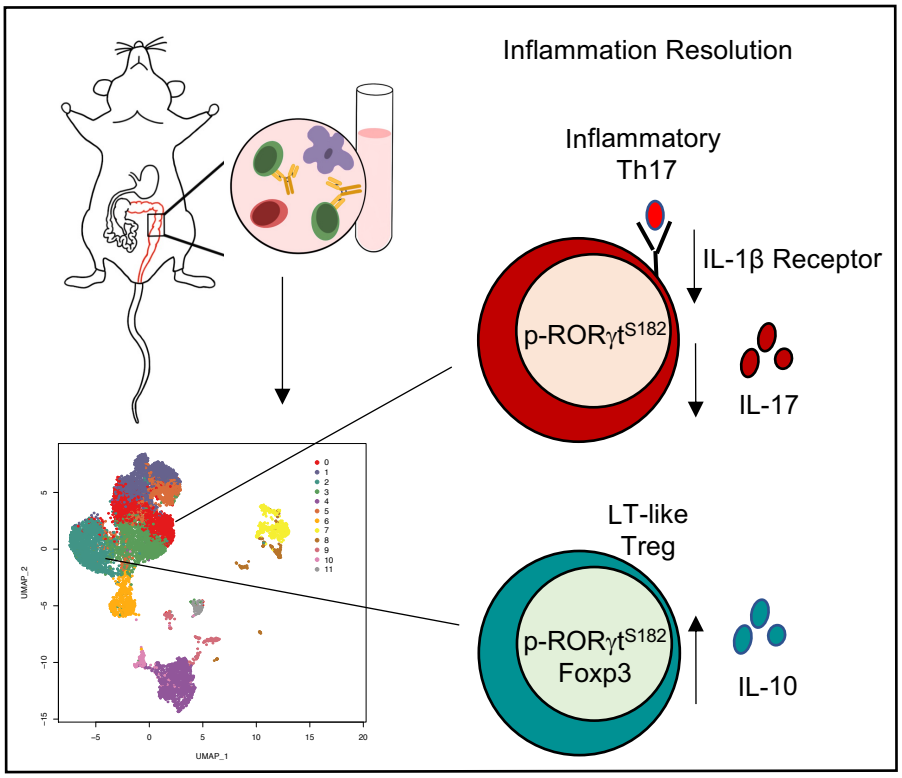

Serine 182 on RORγt limits T cell mediated intestine and central nervous system inflammation.

Highlights

- Single-cell RNA-seq of the colonic lamina propria reveals CD4^{+} T cell heterogeneity under steady state and during dextran sulfate induced colitis.
- The master transcription factor RORγt of Th17 and Treg cell functions is phosphorylated at serine 182.
- Serine 182 on RORγt represses IL-1β-induced IL-17A production in in Th17 cells and potentiates IL-10 production in colonic LT-like Treg cells.
- Phospho-null RORγt^{S182A} mice succumb to exacerbate inflammation when challenged in models of colitis and experimental autoimmune encephalomyelitis.

Fig 1. **scRNA-seq revealed RORγt^{S182} dependent Th17 and Treg populations in steady state colon.**

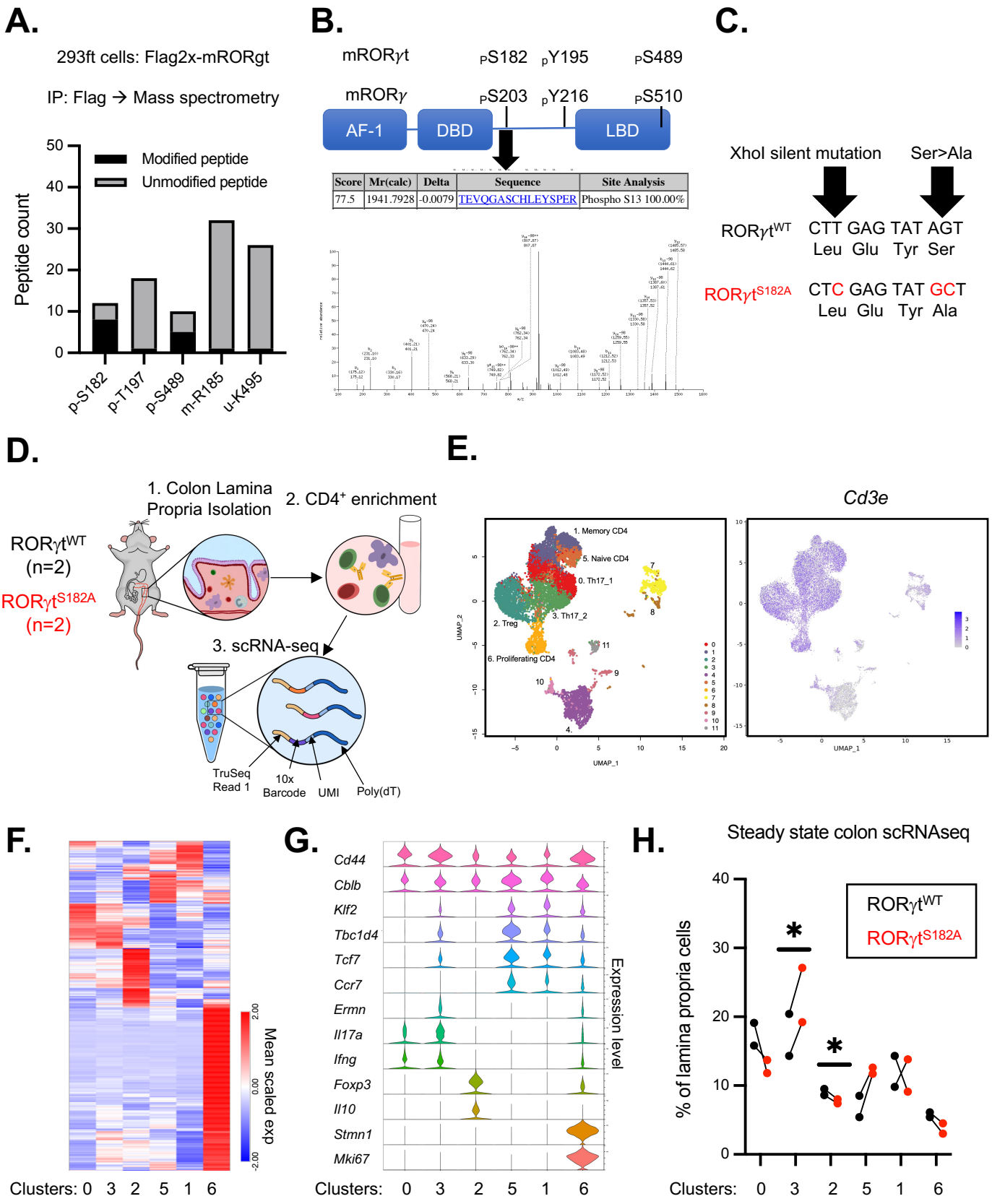

Fig 2. **scRNA-seq identified two subsets of Th17 cells in the steady state colon.**

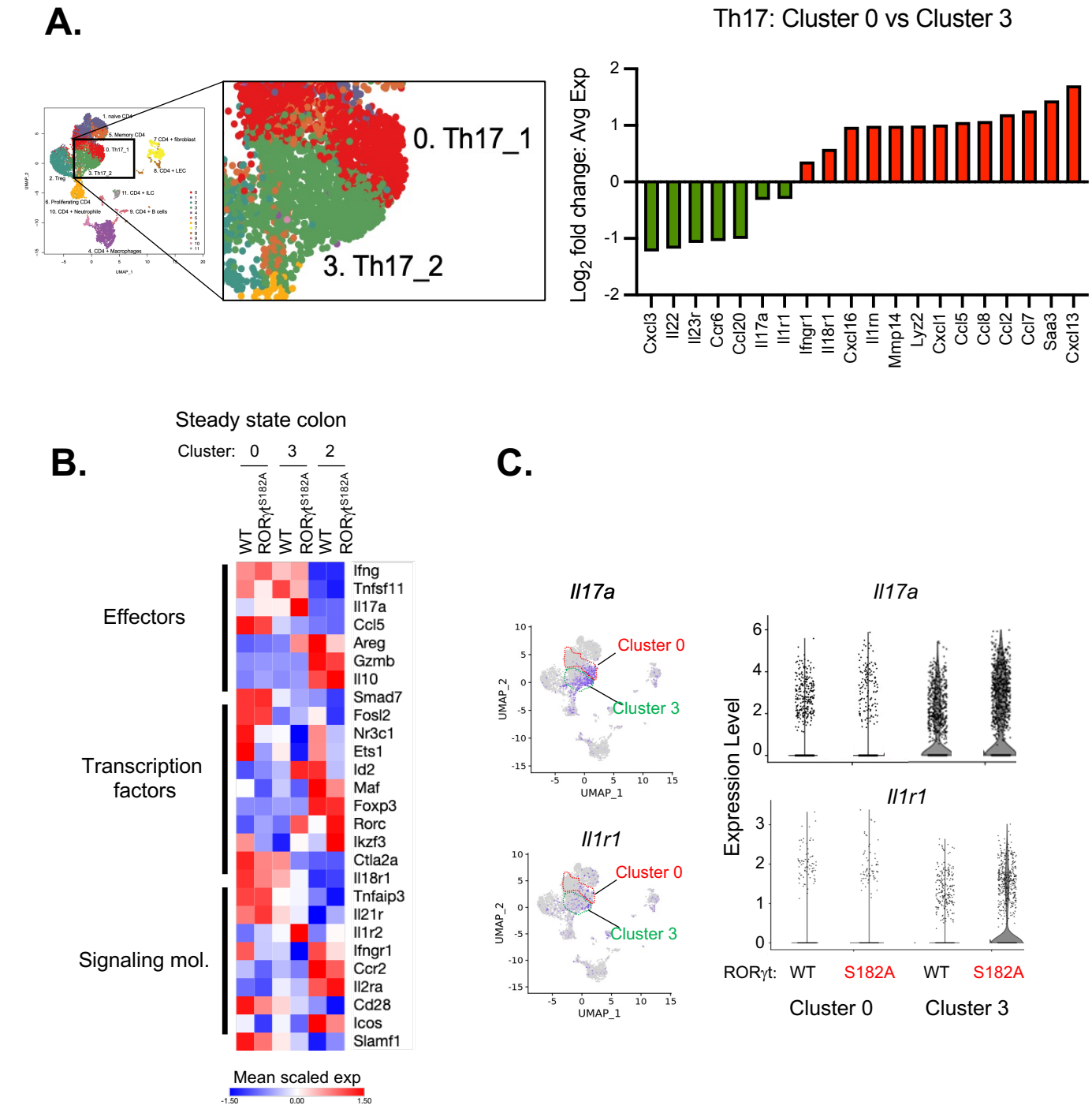

Fig 3. **IL-1β signaling promoted dysregulated effector cytokine production in RORγt^{S182A} Th17 cells.**

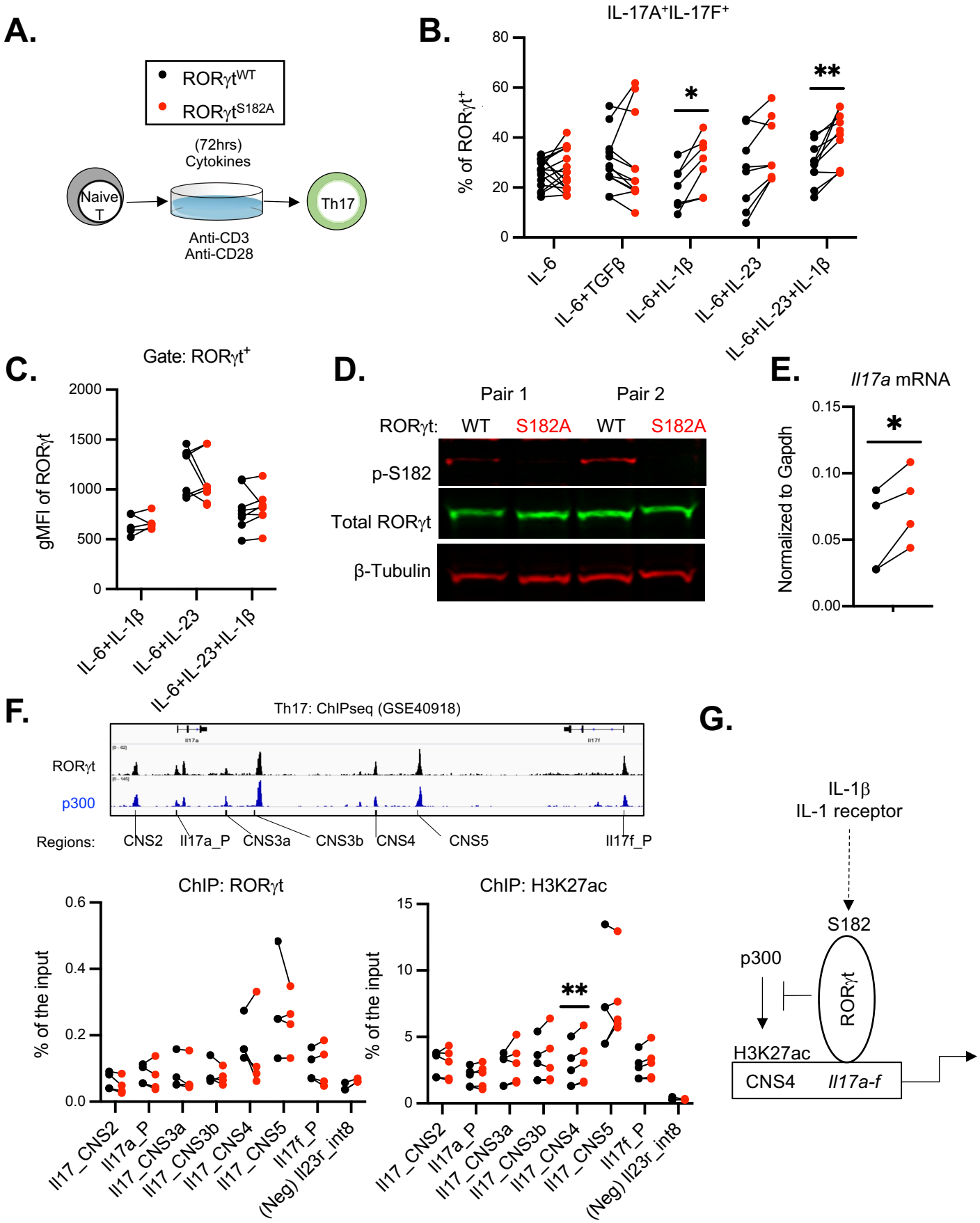

Fig 4. **RORγt^{S182A} T cells drived exacerbated diseases in two models of colitis.**

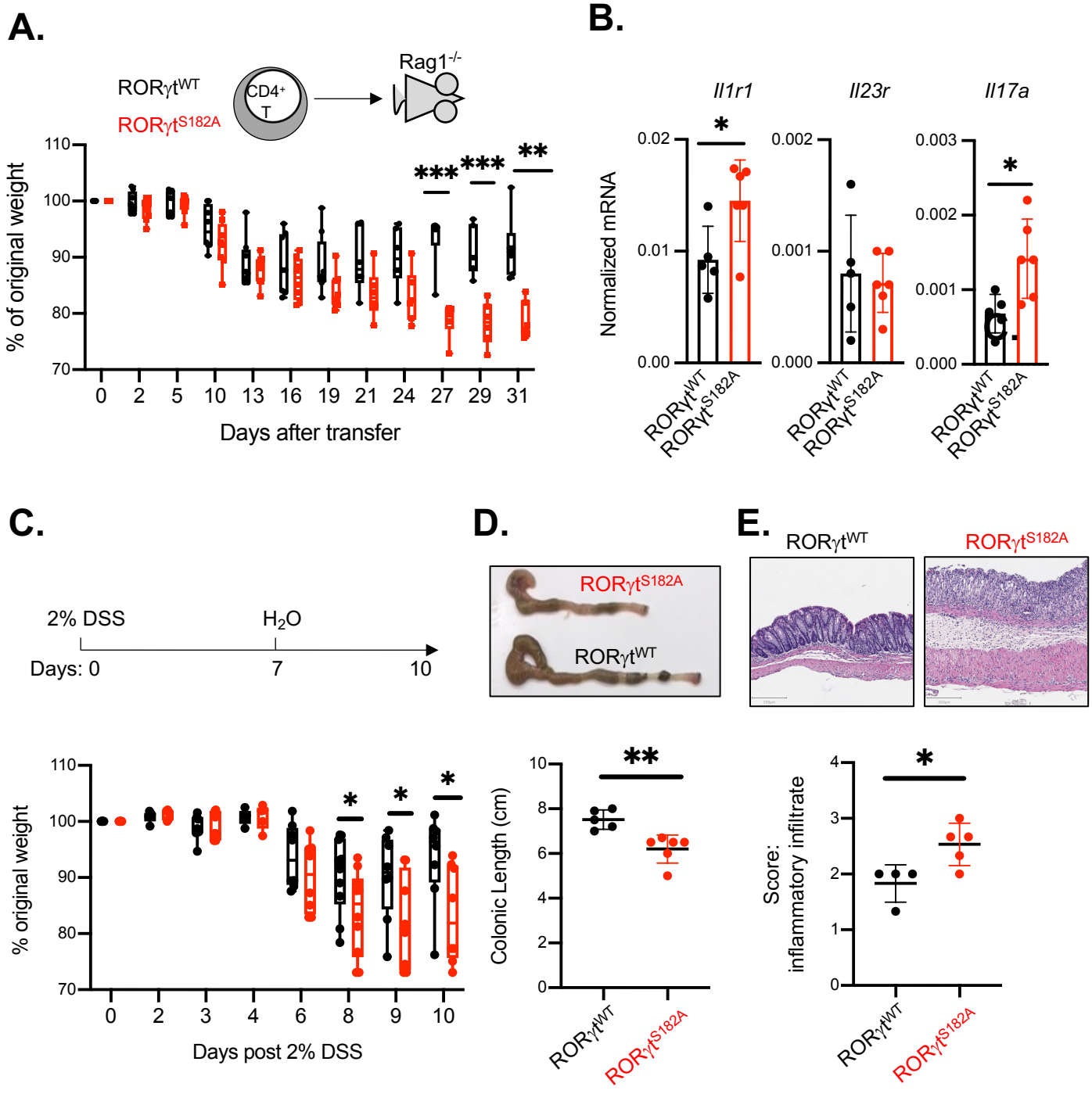

Fig 5. **scRNA-seq revealed RORγt^{S182}-dependent colonic Th17 and Treg programs during DSS challenge.**

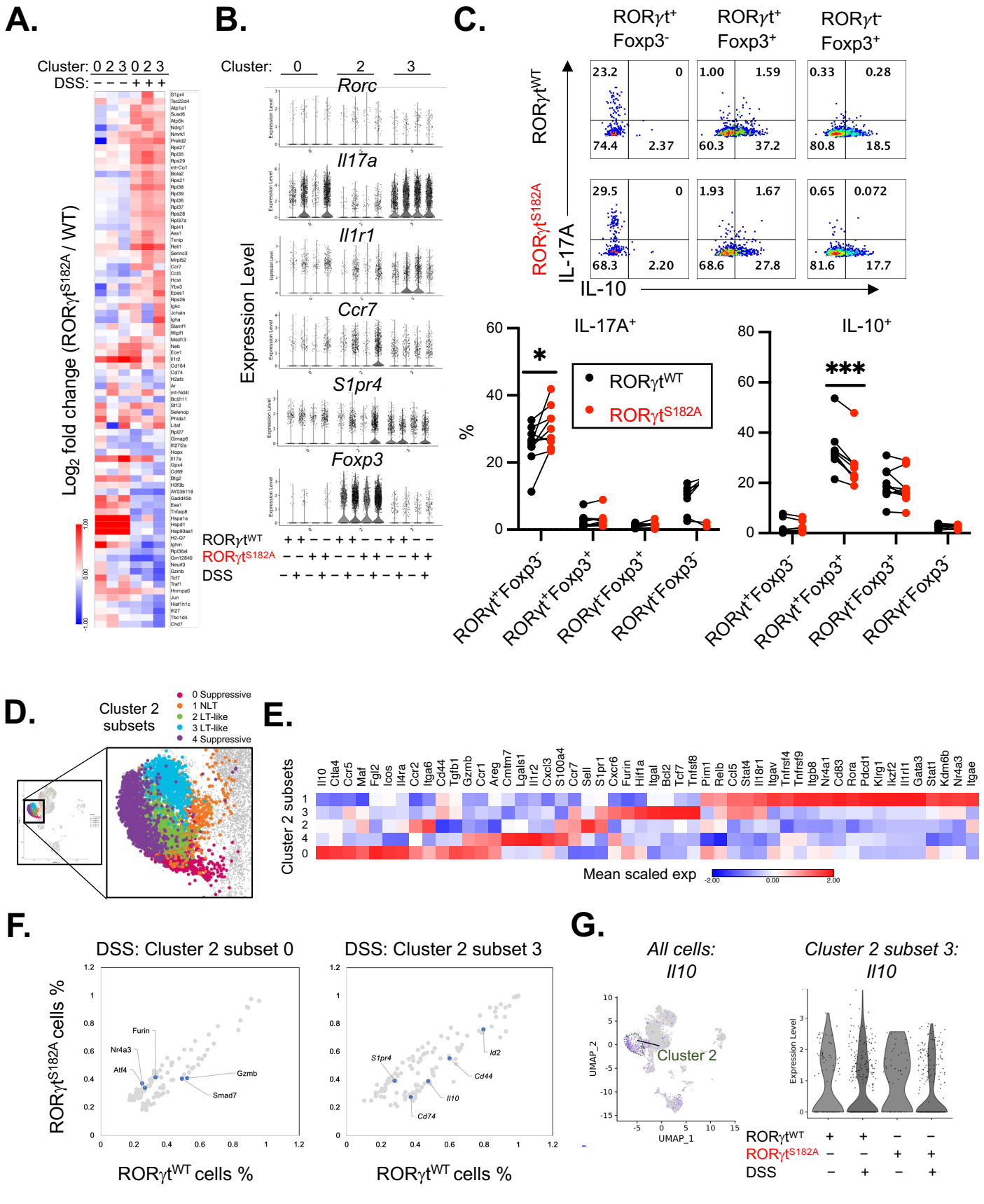

Fig 6. **RORγt^{S182A} mice experienced more severe disease in EAE model.**

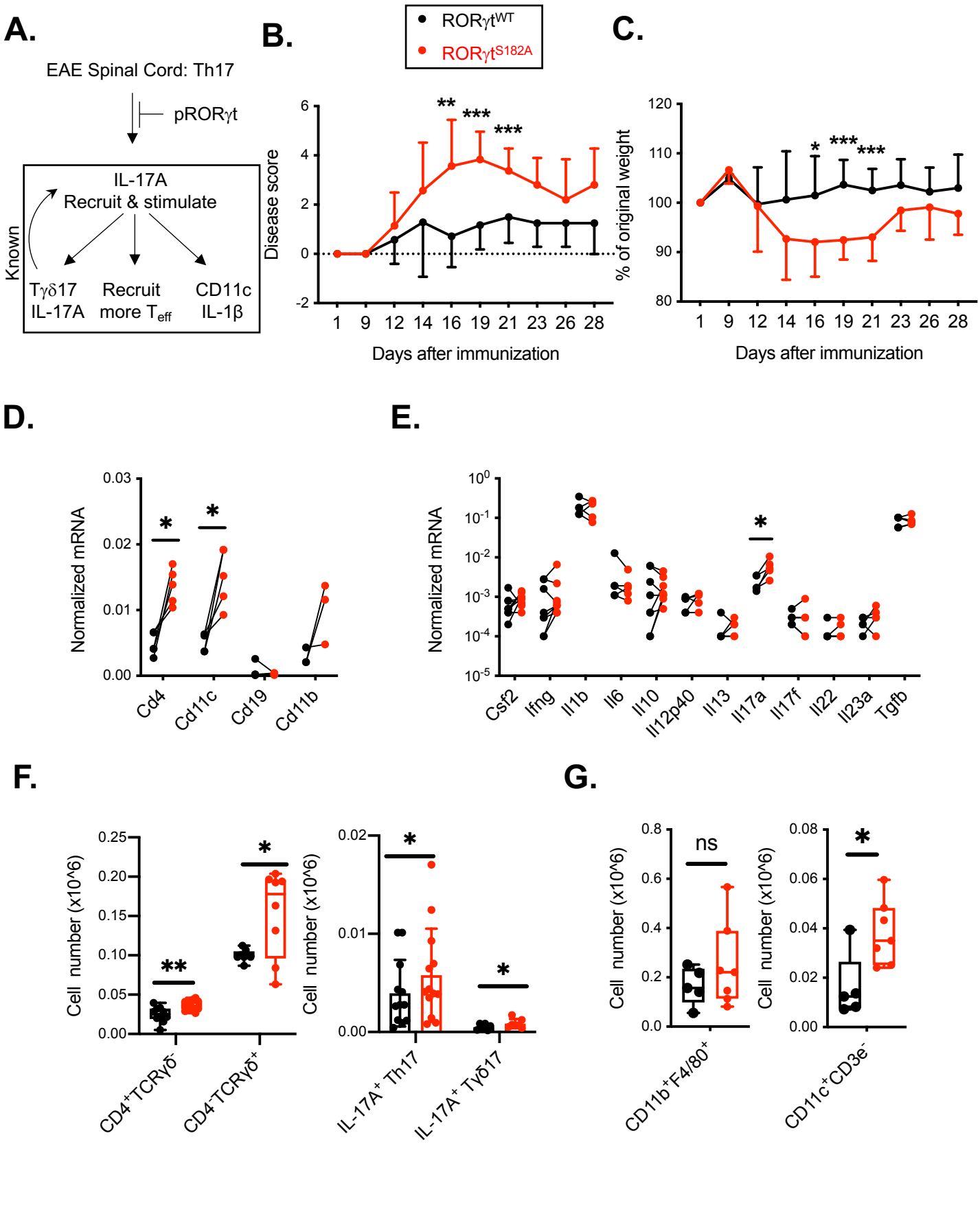

Supplementary

Fig S1. **Normal thymic T cell development and intestine homeostasis in RORγt^{S182A} mice.**

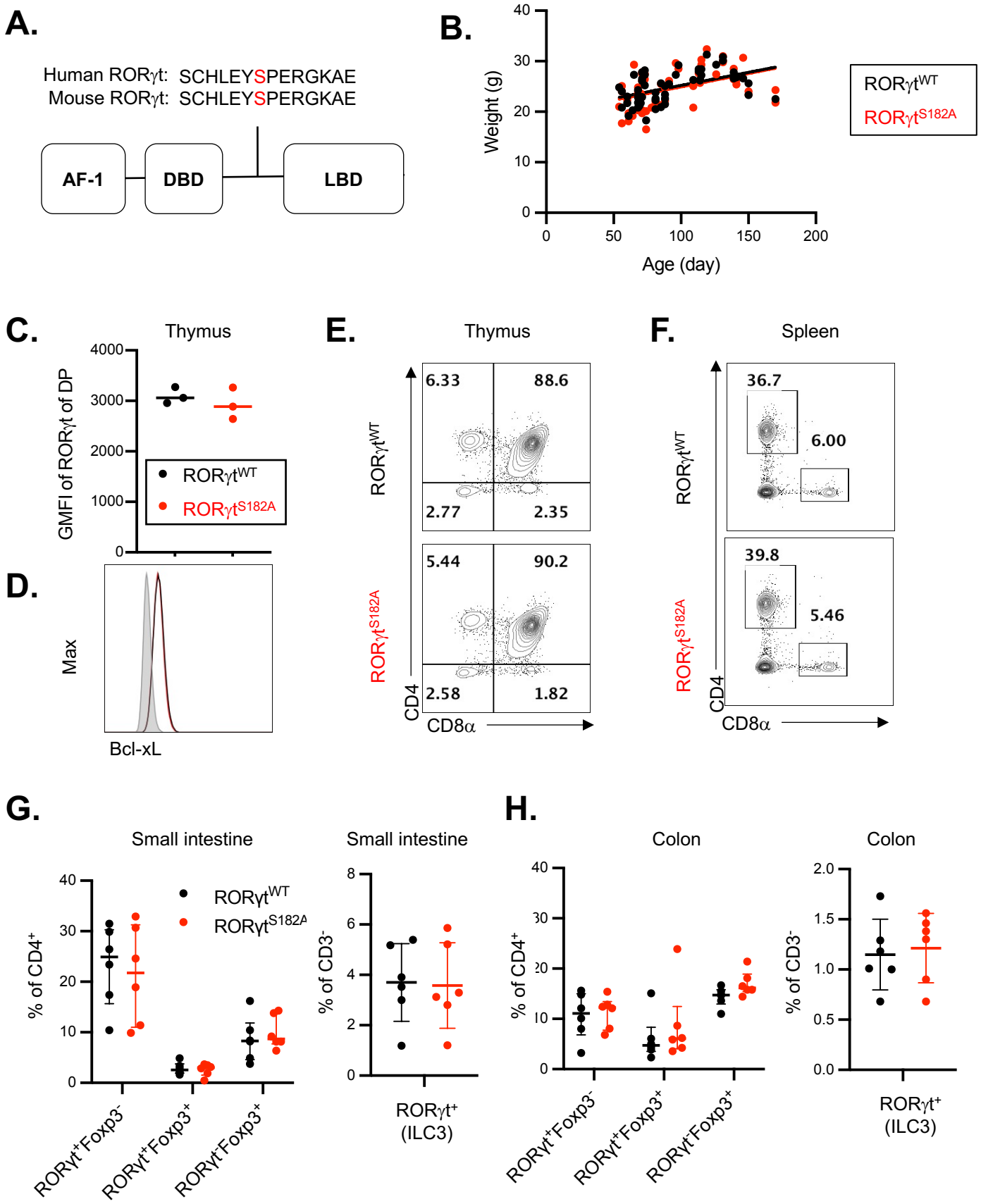

Fig S2. **Representative cytokine production potential in Th17 cells cultured from WT and RORγt^{S182A} mice.**

A.

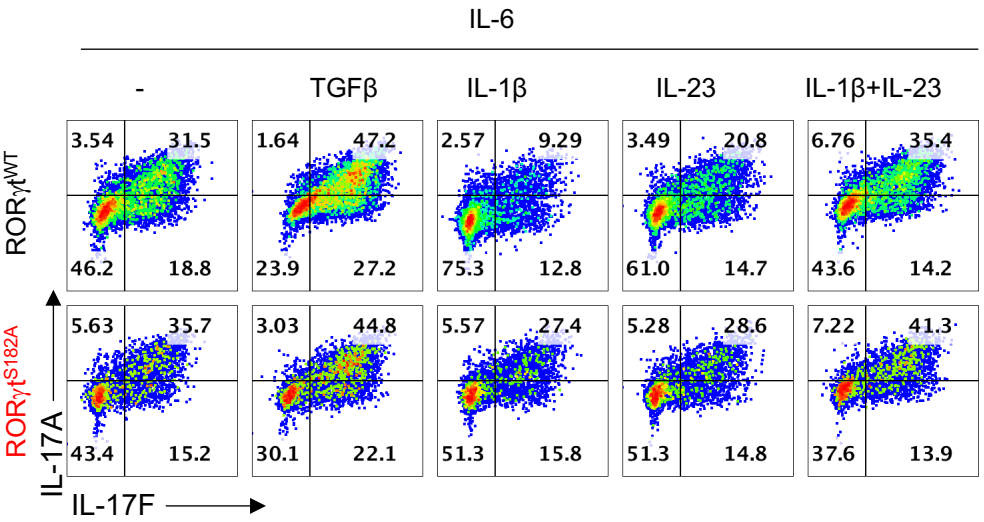

Fig S3. **Cell surface IL-1R expression on colonic Th17 cells in steady state and DSS-challenged WT and RORγt^{S182A} mice.**

A.

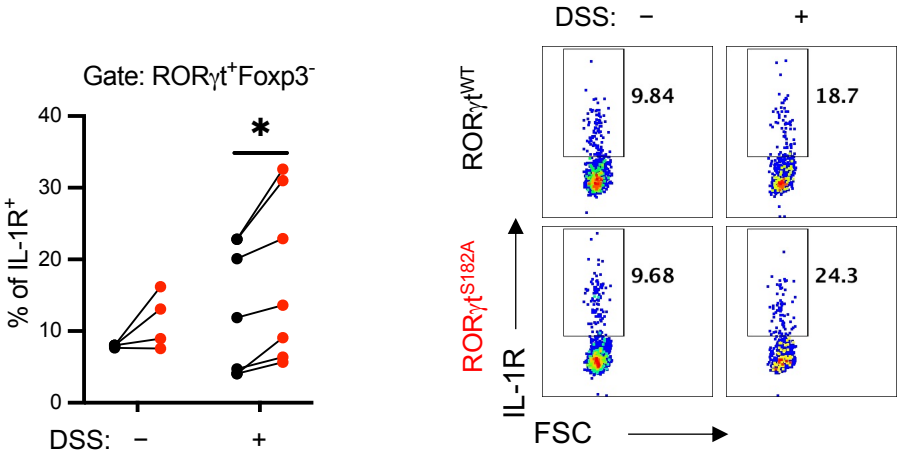

Fig S4. **DSS-induced epithelial injury altered colonic immune cell populations and their transcription programs in WT mice.**

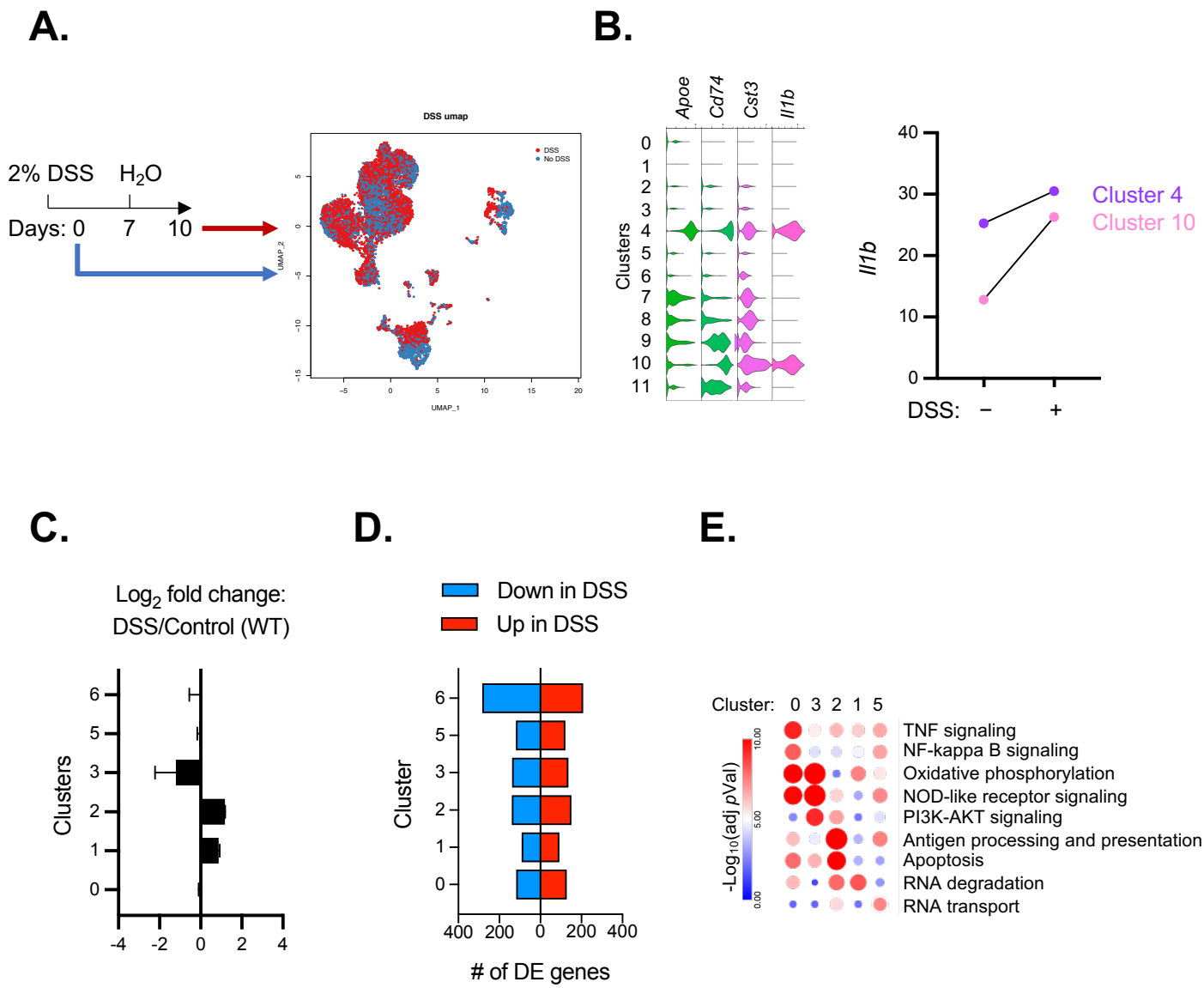

Fig S5. **RORγt^{S182}-dependent cell populations and target genes in colon under steady state and during DSS challenge.**

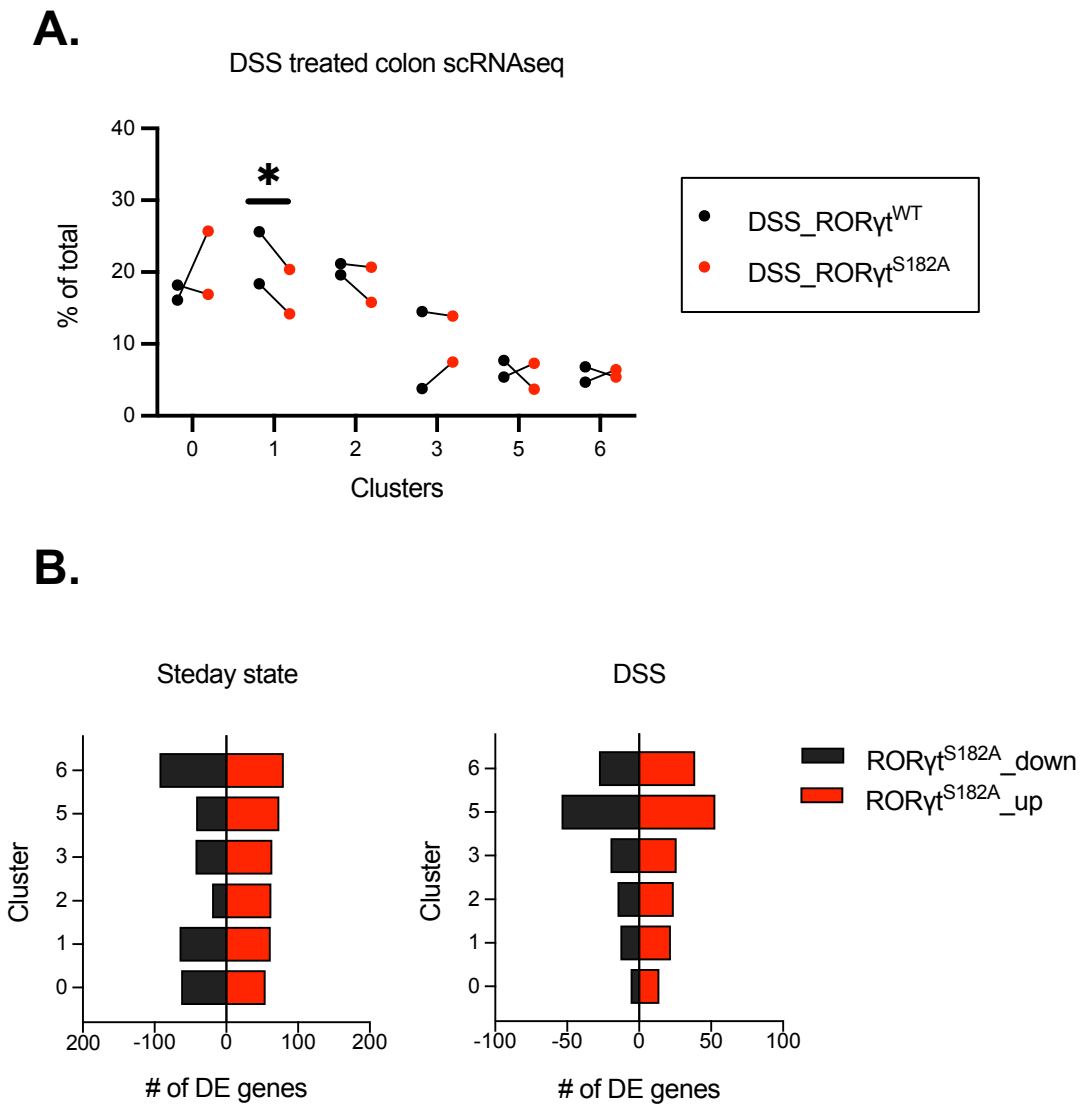

Fig S6. **Cluster 2 Treg subsets in control and DSS-challenged WT and RORγt^{S182A} mice.**

A.